nature communications

Article

https://doi.org/10.1038/s41467-025-60354-8

Electrochemical deprotonation of halohydrins enables cascading reactions for CO_2 capture and conversion into ethylene carbonate

Received: 6 November 2024

Accepted: 21 May 2025

Published online: 30 May 2025

Check for updates

Jeong Hyun Kim[1,2], Young In Jo[1,2], Jun Ho Jang[1,2], Hyun Ji Yu[1], Jeong Eun Kim[1], Hyun Jae Kim[1], Jia Bin Yeo[1], Moo Young Lee[1] & Ki Tae Nam[1]

Electrochemical processes for CO_2 mitigation can be broadly categorized into two approaches: CO_2 capture via electrochemically generated bases and CO_2 conversion through electrochemical reduction. Recent advancements have been concentrated to developing methods that efficiently capture and release CO_2 or reduce base-CO_2 adducts while regenerating bases for subsequent CO_2 capture. In this study, we introduce an electrochemical strategy that integrates CO_2 capture and conversion through a series of domino reactions initiated by the electrochemical generation of organic bases. This method involves the electrochemical deprotonation of halohydrin molecules, which generate hydrogen and halo-alkoxides that capture CO_2 and spontaneously undergo intramolecular cyclization to yield cyclic carbonates. Direct and indirect Faradaic efficiency of up to 100% is achieved for both hydrogen and ethylene carbonate production, demonstrating highly selective sequential capture and conversion reactions. Our system provides a scalable pathway for synthesizing various cyclic carbonates directly from diluted CO_2 sources.

In the pursuit of achieving net-zero emissions alongside escalating energy demands, integrating carbon capture, utilization, and storage (CCUS) technology into conventional fossil fuel-based energy production processes is imperative. Representative technologies such as amine scrubbing[1], and CO_2 hydrogenation[2] rely on thermal processes for both capture and utilization. Recently, electrochemical processes have emerged as promising alternatives, offering potential advantages such as enhanced energy efficiency, adaptability to decentralized operations, and compatibility with renewable energy sources. Electrochemical processes can be adopted for both CO_2 capture and conversion by designing reactions that generate bases, capable of capturing CO_2 or facilitate the reduction of CO_2[3].

For example, the typical approach in electrochemical CO_2 capture (ECC) involves utilizing cathode reactions to produce alkaline species capable of capturing CO_2, and anode reactions for CO_2 release[4,5]. ECC aims to enhance the energy efficiency of the capture and release processes compared to conventional amine scrubbing[6–9], thus necessitating the selection or design of facile redox reactions that ensure high selectivity and low overpotential. In this regard, quinones and its derivatives have been extensively researched as effective redox-active CO_2 carriers owing to their highly reversible redox kinetics[10,11]. Additionally, various selectively occurring half-reactions have been coupled in ECC, such as HER/OER (Hydrogen Evolution Reaction/Oxygen Evolution Reaction) and ORR/OER (Oxygen Reduction Reaction/Oxygen Evolution Reaction)[12,13].

Coupling the reduction reactions of base-CO_2 adducts, such as carbonates/carbamates, with the OER can represent a promising approach to achieving the simultaneous electrochemical conversion

[1]Department of Materials Science and Engineering, Seoul National University, Seoul, Republic of Korea. [2]These authors contributed equally: Jeong Hyun Kim, Young In Jo, Jun Ho Jang. e-mail: nkitae@snu.ac.kr

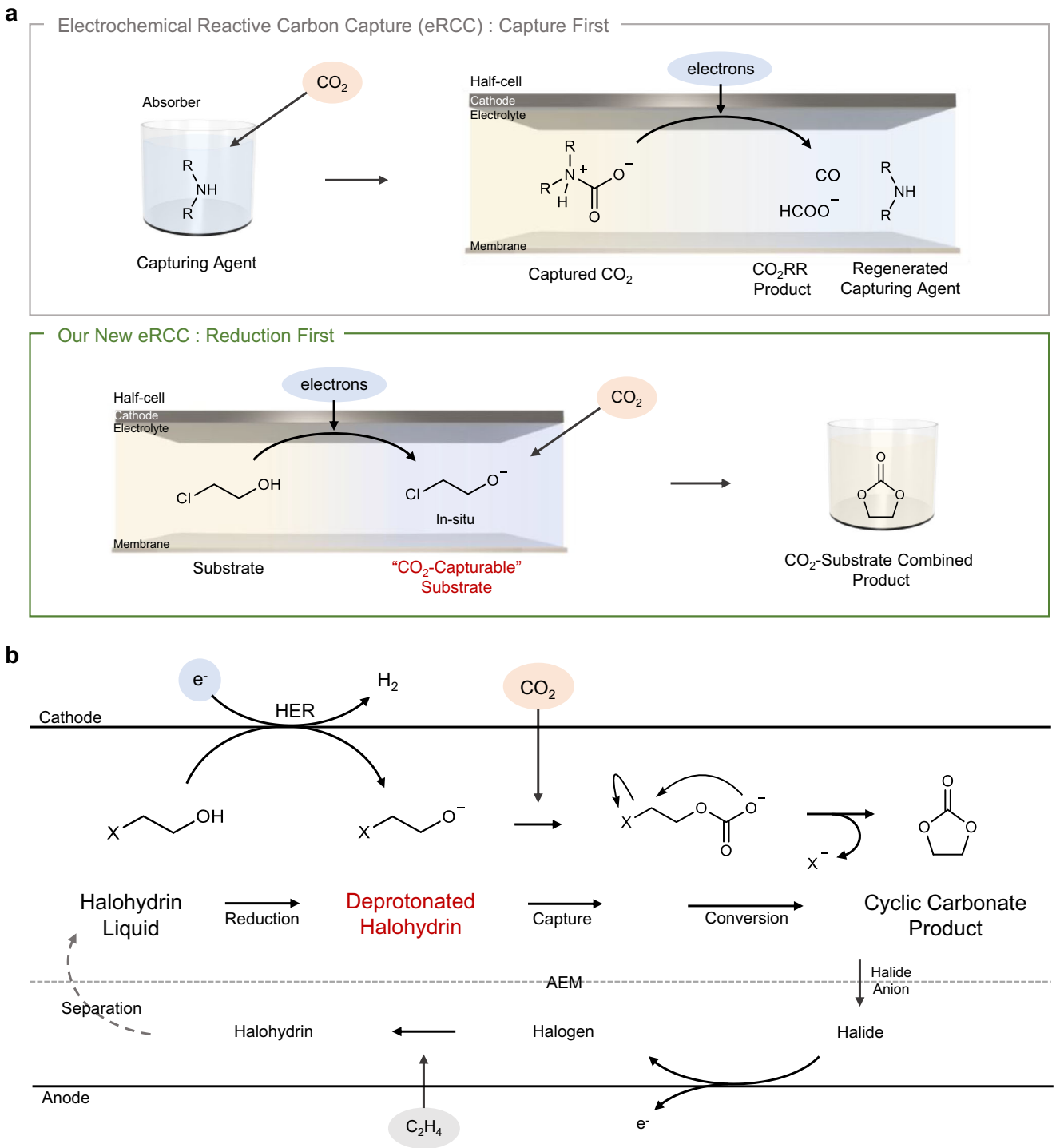

Fig. 1 | Our new eRCC system for the electrosynthesis of CO_2-inserted cyclic carbonate. a Schematic of the conventional electrochemical Reactive Carbon Capture (eRCC) and our new eRCC system. In the conventional eRCC system, CO_2 capture by the capturing agent precedes, and electrons are supplied to the captured CO_2 molecule to electrochemically reduce CO_2 and simultaneously regenerate the capturing agent. In contrast, in our new eRCC system initially supplies electrons to the substrate, followed by CO_2 capture by the produced CO_2-capturable substrate. The captured CO_2 then cascades into a CO_2 conversion reaction, resulting in a CO_2-substrate combined product. The colors of the liquids were selected to indicate their basicity: a light yellow color represents a neutral pH, while a pale blue color represents a basic pH. A darker blue color was chosen for haloalkoxides to indicate that they are more basic than amine species. **b** Schematic representation of the electrochemical cyclic carbonate synthesis system. Through electrochemical deprotonation, halohydrin becomes capable of capturing CO_2, leading to an intermediate that cascades into a cyclic carbonate. The leaving group detached from the conversion reaction is used at the counter electrode to synthesis halohydrin.

of CO_2 and production of bases for CO_2 capture[14]. This approach, known as electrochemical reactive carbon capture (eRCC), involves introducing electrons to chemisorbed CO_2 species like carbamates and carbonates, resulting in CO_2 reduction products (e.g. CO, formate, etc.) while restoring the basicity of the solution[15–17] (Fig. 1a). However, the electrochemical reduction of carbonates and carbamates often exhibits low energy efficiency compared to ECC due to competing HER and sluggish kinetics. A desirable research direction would involve

exploiting the advantage of ECC systems featuring highly selective redox reactions, while concurrently accomplishing CO_2 conversion. We thought that this could be achieved if the CO_2 captured with electrochemically generated bases could spontaneously transform into stable, value-added chemicals without requiring further reduction of the chemisorbed CO_2 species, the goal of combining CO_2 capture via highly selective redox reactions with concurrent conversion could be achieved. For instance, deprotonation of an organic proton donor via cathodic HER could yield an organic base. If the organic base-CO_2 adduct formed during CO_2 capture is reactive in subsequent intra- or inter-molecular reactions, we expect to construct a new electrochemical system that captures and converts CO_2 simultaneously through facile half-reactions.

Halohydrins are potential candidates as organic proton donors for such systems, because halohydrins could yield halo-alkoxides upon deprotonation, which can react with CO_2 to form halo-alkoxide-CO_2 adducts. These adducts can then spontaneously transform into cyclic carbonates through intramolecular cyclization reactions[18]. This unique property of halohydrins has been leveraged in prior studies[19–22], using an equivalent amount of base to deprotonate the alcoholic protons of halohydrins under a CO_2 atmosphere, thereby producing cyclic carbonates. Recently, our group proposed an electrochemical version where CO_2 is first captured as bicarbonate with electrochemically generated bases, which is then utilized as a CO_2 donor and base for synthesizing ethylene carbonate in a subsequent step[23]. Based on this study, we explore the possibility that direct electrochemical deprotonation of halohydrins via HER could eliminate the need for a separate deprotonating agent and an additional conversion step, thereby simplifying the overall process of CO_2 capture and conversion using halohydrins.

With this motivation, we report a new electrochemical strategy wherein an electrogenerated halo-alkoxide base captures CO_2 and simultaneously transforms into cyclic carbonate. Specifically, the electrochemical reduction deprotonates halohydrins, concurrently generating hydrogen and halo-alkoxides that function as CO_2 capturing bases. The resulting halo-alkoxide-CO_2 adducts undergo spontaneous intramolecular cyclization reactions to form cyclic carbonates (Fig. 1a). We observed maximum Faradaic efficiency of nearly 100% for HER and an indirect Faradaic efficiency of nearly 100% for ethylene carbonate production under CO_2 atmosphere, successfully validating our new concept. For efficient ethylene carbonate production, careful selection of the halogen leaving group and supporting electrolyte cation were important. In addition, by facilitating CO_2 mass transfer with gas diffusion electrodes and co-solvent, our system demonstrated operation under diluted CO_2 concentrations (1.5% and 15%) with ethylene carbonate production efficiency of 50% and up to 100%, respectively. Production of various cyclic carbonates with vicinal halohydrins confirmed the expandability and generality of this reaction scheme.

Result

Concept validation

Figure 1b illustrates our scheme of chemical and electrochemical reactions. The design involves performing the HER at the cathode and the halogen evolution reaction at the anode. In the cathodic compartment, electrochemical deprotonation of halohydrin simultaneously generates hydrogen, cyclic carbonate, and a halide anion. An anion exchange membrane (AEM) can be introduced to prevent product crossover while facilitating the migration of the halide anion towards the anodic compartment[24], where it replenishes the halide consumed at the anode as a reactant for the halogen evolution reaction. Our ionic circuit is more specifically described in Supplementary Fig. 1. Note that the produced halogen can be utilized as a reactant for the preparation of halohydrins.

To validate the designed concept, bulk electrolysis was conducted using a two-compartment, membrane-separated cell (Fig. 2a). In the cathodic compartment, a 0.5 M tetrabutylammonium chloride solution (TBACl) in chloroethanol was used as the catholyte, with CO_2 gas bubbled through the solution to ensure saturation prior to the experiment. 2-Chloroethanol was chosen because it is an ethylene halohydrin derived from ethylene, the smallest molecule containing a C=C double bond, providing a fundamental model for investigation. Pure halohydrin liquid was used as a solvent as well as a reactant to minimize the potential side reactions. For the anodic compartment, three different anolytes were evaluated: 0.5 M NaCl in water, 0.5 M TBACl in acetonitrile, and 0.5 M TBACl in chloroethanol. Ethylene carbonate was consistently detected in the catholyte in all cases (Supplementary Fig. 2). The overall cell resistance was the lowest with the aqueous anolyte (Supplementary Table 1), despite the presence of a liquid junction between the two solvents. In addition, when using an aqueous anolyte, supplying ethylene gas to the anodic compartment resulted in the generation of halohydrin through the reaction with the produced halogen and water (Supplementary Fig. 3). Before selecting the aqueous anolyte, we assessed the potential risk of water penetration through the membrane affecting the cathode reaction by comparing a 2-chloroethanol catholyte with intentionally added water (Supplementary Figs. 4, 5). The results showed that water crossover does not noticeably impact the cathode reaction.

Using the aqueous anolyte with the CO_2-saturated chloroethanol catholyte, we tested three cathodes: Pt, Ni, and Au plates. Post-electrolysis, we observed high selectivity for HER at the cathode, along with the production of ethylene carbonate (Fig. 2b). The HER faradaic efficiency was nearly 100% for Pt and Ni, while slightly lower for Au (~90%). To quantify ethylene carbonate's yield, we introduced the term indirect Faradaic efficiency (iF.E.), defined as:

$$\text{Indirect Faradaic Efficiency(iF.E.)} = \frac{\text{Total produced ethylene carbonate}\,[\text{mol}]}{\text{Supplied electrons}\,[\text{mol}]} \times 100\% \quad (1)$$

The concept of Faradaic efficiency typically describes the efficiency of charge transfer in an electrochemical system. However, in the electrochemical synthesis of ethylene carbonate, no change occurs in the redox state of the involved atoms. Instead, ethylene carbonate is formed indirectly via chemical reactions involving electrochemically generated species. To account for this, we define iF.E. as a measure of the charge utilization efficiency leading to ethylene carbonate formation. The maximum theoretical iF.E. corresponds to the direct electroreduction of the halohydrin's O-H bond, as illustrated in Fig. 1b, where one molecule of ethylene carbonate is produced per supplied electron. Conversely, the indirect Faradaic efficiency for ethylene carbonate was highest with Au (~70%) and similar for Pt and Ni (~60%). Considering Au's efficacy as a catalyst for the selective reduction of CO_2 to CO[25], the slight reduction in HER efficiency is likely due to the undesired CO_2 reduction reaction. Additionally, the selective binding of CO_2 on the Au electrode[26] might contribute to the increased production of ethylene carbonate. Importantly, in all cases, the sum of the Faradaic efficiency for HER and indirect Faradaic efficiency for ethylene carbonate exceeded 100% and isotopic labeling experiments verifying that hydrogen is sourced from electrochemical deprotonation of -OH (Supplementary Fig. 6). These results indicate that ethylene carbonate production is a consequence of alkoxide anion generation during HER. In the absence of CO_2 in the catholyte, ethylene oxide was produced (Supplementary Figs. 7, 8), which further confirmed the generation of alkoxide anion[27]. Notably, the difference between the Faradaic efficiency for H_2 and the indirect Faradaic efficiency for ethylene carbonate correlates with the formation of ethylene oxide. This correlation arises because the production of H_2 indicates the generation of halo-alkoxide, with one halo-alkoxide formed per electron, and the difference corresponds to the conversion of halo-alkoxide to ethylene carbonate via self-ring closure. Although ethylene oxide was not quantified due to its volatility, it was detected in the

https://doi.org/10.1038/s41467-025-60354-8

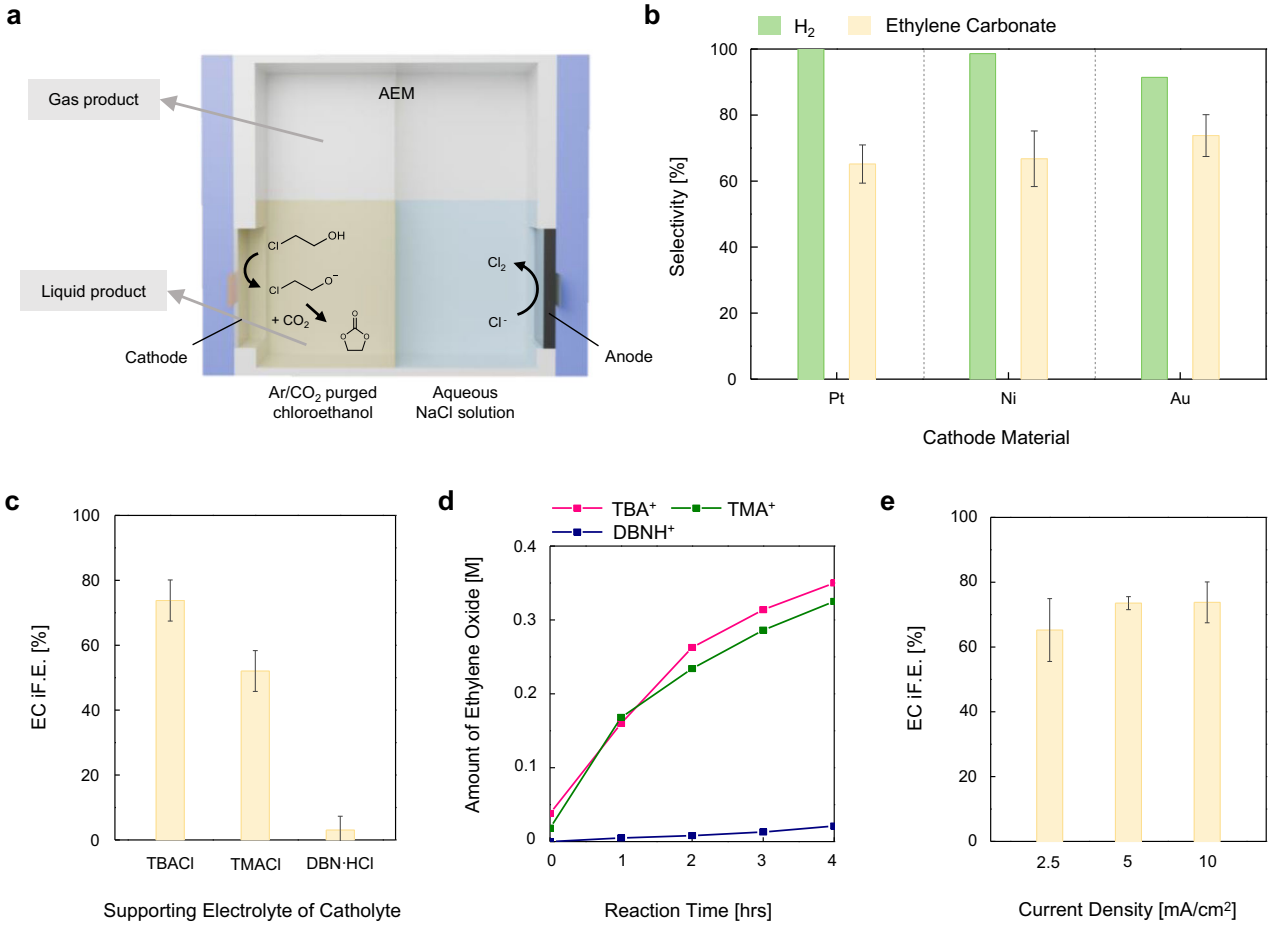

Fig. 2 | Concept verification and electrochemical investigation of the system components. a Schematic depiction of the electrochemical cell setup. Before the electrochemical reaction, either argon or CO_2 gas was bubbled into the catholyte. The cell remained closed during the reaction. Gas and liquid products were analyzed using gas chromatography and NMR spectroscopy, respectively. **b** Selectivity of the cathode reaction among products using three different cathode materials. The left columns in each group indicate the selectivity of H_2 among gas products from an Ar-saturated catholyte. The production of H_2 suggests that halohydrin was electrochemically reduced to produce alkoxide. The right columns in each group show the average selectivity of EC by Faradaic efficiency in a CO_2-saturated catholyte. The selectivity of ethylene carbonate was repeatedly measured three times, and the error bars indicate standard deviation. **c** Average EC iF.E. values with three different supporting electrolytes. To investigate the cationic effect, tetraalkylammonium salts with different carbon chain lengths and amidine salt were compared under same current densities of 10 mA/cm^2. Each point was repeatedly measured three times, and the error bars indicate standard deviation. **d** Amount of ethylene oxide generated over time from the reaction between 2-chloroethanol and three different bases. To investigate the cationic effect on the alkoxide, combinations of the cation corresponding to the salt used in **c** and hydroxide anion were used as the base. The reaction was carried out in a 0.5 M chloride salt of the corresponding cation-deuterated methanol solution. **e** Average EC iF.E. values at three different current densities (2.5, 5, 10 mA/cm^2). Each point was repeatedly measured three times, and the error bars indicate standard deviation. Source data for Fig. 2b, c–e are provided as a Source Data file.

post-electrolysis solution containing CO_2 (Supplementary Fig. 7). However, its concentration was substantially lower compared to the solution without CO_2. Additionally, there was no significant presence of products other than ethylene carbonate and ethylene oxide.

Effect of electrolyte and current on EC selectivity

To investigate the effect of surrounding cations on ethylene carbonate production, we tested three different supporting electrolytes. Tetraalkylammonium cations resulted in significantly higher indirect Faradaic efficiency, while the protonated amidine cation showed considerably lower efficiency (Fig. 2c). Among the tetraalkylammonium cations, the indirect Faradaic efficiency increased with the size of the cation. We hypothesized that a cation-alkoxide interaction could explain this observed difference in efficiency. To explore the extent of cation-alkoxide interaction, we compared the rate of ethylene oxide production in each cationic environment. 2-Chloroethanol was chemically deprotonated using organic hydroxide in the presence of different cations, and the amount of ethylene oxide produced was measured at intervals. The results showed that the rate of ethylene oxide formation was much higher in the presence of tetraalkylammonium cations compared to the protonated amidine cation (Fig. 2d). This indicates that the interaction between tetraalkylammonium cations and the alkoxide is much weaker than that of the protonated amidine cation, leading to faster ring closure. From this data, we think that the higher ethylene carbonate efficiency with tetraalkylammoniums is due to the weaker cation-alkoxide interaction, which would facilitate easier insertion of CO_2.

We also investigated the effect of alkoxide production rate on ethylene carbonate production efficiency by varying the current density (Fig. 2e). The three different current densities resulted in similar indirect Faradaic efficiencies, regardless of their values. This suggests that the CO_2-alkoxide adduction is sufficiently fast and that the rate of ethylene carbonate production is determined by the alkoxide production rate.

Effect of halogen species on EC selectivity

Chloroethanol acts as both the solvent and reactant for hydrogen and ethylene carbonate production. By testing bromo- and iodo-ethanol as

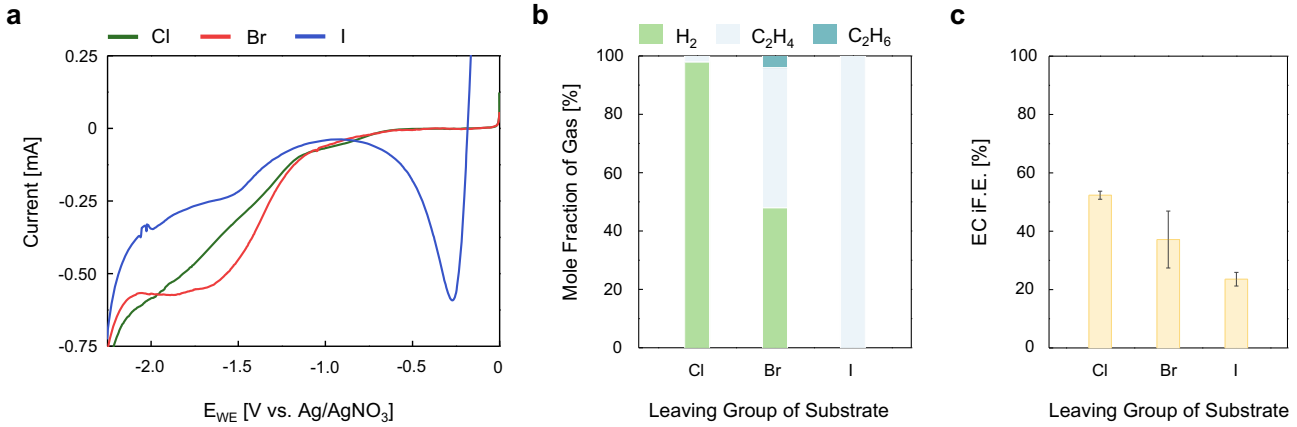

Fig. 3 | Selection of the leaving group of the substrate for efficient cyclic carbonate synthesis. a Cyclic voltammograms of the 50 mM 2-chloroethanol, 2-bromoethanol, and 2-iodoethanol in 0.5 M TBACl-acetonitrile solution. The cathodic reduction of 2-iodoethanol at −0.3 V vs $Ag/AgNO_3$ corresponds to the I_3^-/I^- redox pair[28]. The reduction peaks of 2-iodoethanol and 2-bromoethanol around −1.5 to −1.75 V vs $Ag/AgNO_3$ corresponds to the reduction of carbon-halogen bond. The voltage was iR-corrected. **b** Selectivity of the gas product using three different halohydrins (2-chloroethanol, 2-bromoethanol, 2-iodoethanol) as catholyte. H_2 was less produced when the leaving group of the substrate was better. **c** Average indirect Faradaic efficiency values of ethylene carbonate with three different halohydrins (2-chloroethanol, 2-bromoethanol, 2-iodoethanol) as catholyte, at a 5 mA/cm^2 current density. 2-Chloroethanol showed the highest EC iF.E. value, indicating that the chloride leaving group fits the best for the electrosynthesis of cyclic carbonates from CO_2 and halohydrin. Each point was repeatedly measured three times, and the error bars indicate standard deviation. Source data for Fig. 3a–c are provided as a Source Data file.

alternatives, we think that chloro-alcohols are essential for efficient cyclic carbonate production. Specifically, we observed that using 2-bromo- or 2-iodo-ethanol led to the cathodic reduction of the C-X bond instead of HER, resulting in the production of ethylene or ethane as side products (Supplementary Fig. 9). Cyclic voltammetry with catholytes containing the three different haloalcohols showed no distinct peak for 2-chloroethanol, while 2-bromoethanol and 2-iodoethanol displayed peaks around −1.5 to −1.75 V (Fig. 3a). Gas product analysis revealed substantial production of ethylene and ethane with 2-bromoethanol and 2-iodoethanol (Fig. 3b). The sharp peak at −0.3 V in the voltammogram of 2-iodoethanol is attributed to the I_3^-/I^- redox pair[28]. These results suggest that C-Br and C-I bonds are more prone to electrochemical reduction compared to C-Cl bonds[29]. Interestingly, the indirect Faradaic efficiency of ethylene carbonate production using 2-bromo- and 2-iodo-ethanol decreased, but not as much as expected based on the Faradaic efficiency of HER (Fig. 3c). Notably, while the Faradaic efficiency of H_2 with 2-iodo-ethanol was near zero, ethylene carbonate was still observed (~20%). This can be explained by the fact that the cyclization reaction does not require direct electron injection. Although electrons are consumed for ethylene and ethane production, alkoxide or hydroxide can be generated, which triggers deprotonation and cyclization of haloalcohols (Supplementary Fig. 10). However, considering that HER requires one electron per one alkoxide or hydroxide but ethane and ethylene production require two electrons (Supplementary Fig. 9), and taking into accounts the atomic efficiency of haloalcohols, we found that chloroethanol is the most suitable substrate.

CO_2 capture and EC synthesis using GDE system

To test the applicability of this system for actual CO_2 capturing circumstances, we lowered the CO_2 concentration to 15% and 1.5%. Directly injecting diluted CO_2 steam into the catholyte resulted in a significant decrease in the indirect Faradaic efficiency of ethylene carbonate (Fig. 4a). To enhance CO_2 supply, we employed a gas diffusion electrode (GDE) to deliver CO_2 directly to the interface between the electrode and the electrolyte (Fig. 4b). Figure 4a confirms that using the GDE increases the indirect Faradaic efficiency compared to the injection method, achieving efficient ethylene carbonate synthesis with over 50% even at 1.5% CO_2 concentration. The GDE configuration also enabled operation at higher current densities (Supplementary Fig. 11). Figure 4c shows the indirect Faradaic efficiency at current densities of 10, 25, and 50 mA/cm^2, comparing 100% and 15% CO_2. Unlike under 100% CO_2 conditions, increasing the current density under 15% CO_2 decreased the indirect Faradaic efficiency of ethylene carbonate, indicating that CO_2 becomes the limiting substrate for the cyclization reaction (Fig. 4c). Further lowering the CO_2 concentration to 1.5% at 50 mA/cm^2 also showed that efficiency is controlled by the CO_2 concentration (Supplementary Fig. 12). These results mean that as CO_2 is the limiting substrate at high current densities and in dilute CO_2 streams, enhancing CO_2 supply is crucial for efficient ethylene carbonate production. Introducing the GDE enabled us to synthesize ethylene carbonate with a comparably high yield by directly capturing CO_2 from a mixed gas source.

We also selected specific conditions to show the operational stability of our system: a current density of 50 mA/cm^2 and CO_2 concentration of 15%, which is the typical flue gas concentrations from coal-fired power plant[30]. Figure 4d shows the indirect Faradaic efficiency and concentration of ethylene carbonate synthesized in the electrolyte, and the cell voltage measured during electrolysis. The constant indirect Faradaic efficiency shows the stability of our system. The concentration of ethylene carbonate consistently increased during electrolysis, reaching 0.09 M after 5 h of operation.

Expansion of substrate scope

A variety of cyclic carbonates are utilized as value-added chemicals, particularly as polymer precursors[31,32], lubricants[33], solvents[34], and additives in battery electrolytes[35]. Since our system relies on facile HER on halohydrin substrates, our strategy could potentially be applied to synthesize various cyclic carbonates. The linear sweep voltammograms of these vicinal chlorohydrin candidates appeared similar to that of 2-chloroethanol, exhibiting HER onset around −2.0 V and no noticeable reduction peak (Supplementary Fig. 13), indicating the viability of expanding the substrate scope. Additionally, H_2 production from vicinal halohydrin was confirmed with gas chromatography (Supplementary Fig. 14). We conducted bulk electrolysis using a two-compartment, membrane-separated cell. As the black line indicates, when the halohydrins were used, cyclic carbonates were synthesized with a low yield of under 10% Faradaic efficiency (Fig. 5). Given that

https://doi.org/10.1038/s41467-025-60354-8

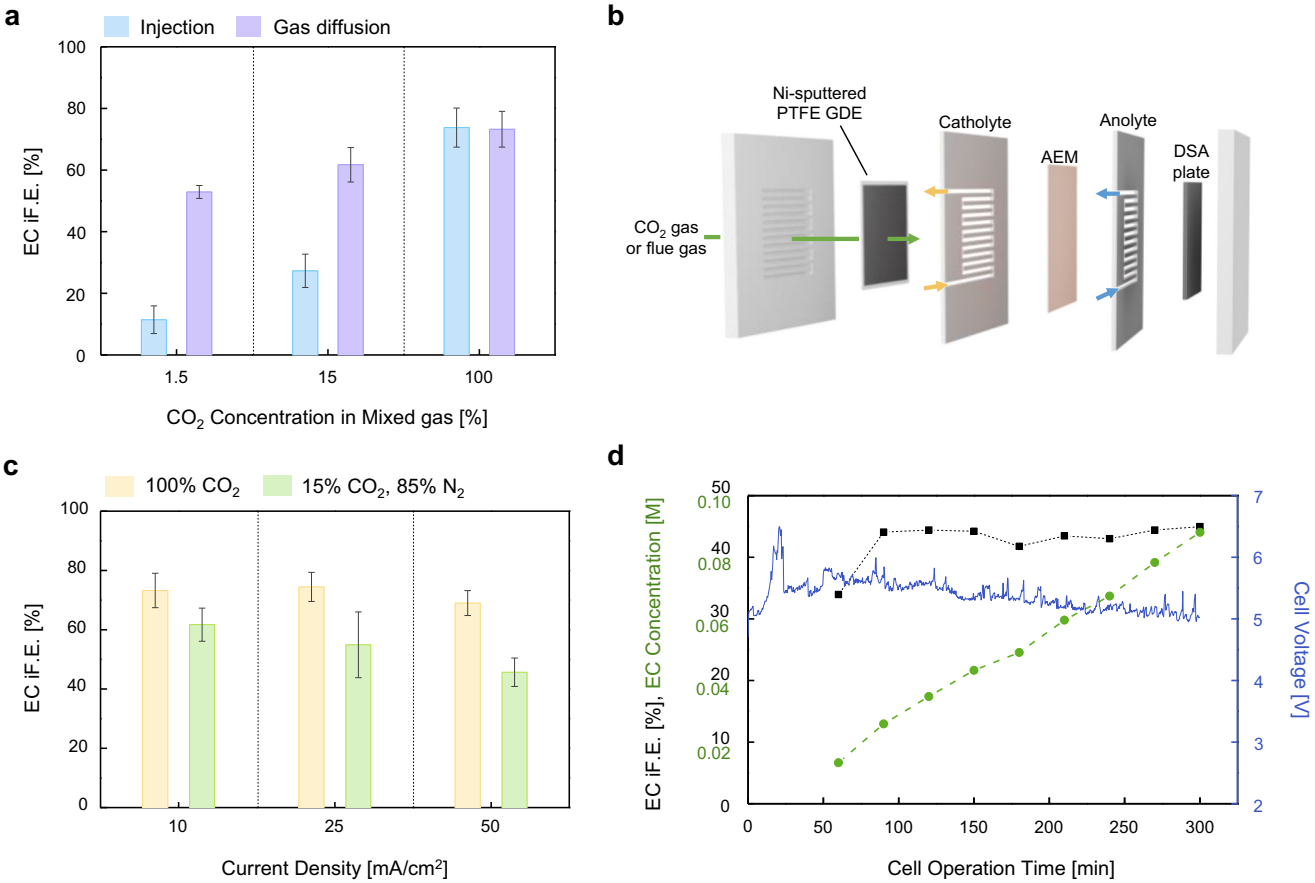

Fig. 4 | Ethylene carbonate synthesis using a gas diffusion electrode and flow cell. a Average indirect Faradaic efficiency values of ethylene carbonate at 10 mA/cm^2 current density using three different compositions of gas (1.5%, 15%, and 100% CO_2, the mixed gases were balanced with N_2), different CO_2 supply methods, and cell constructions. The left columns of each group show the EC iF.E. values in an H-cell, where CO_2 was supplied by injecting it with a needle for 25 min at a gas flow rate of 200 sccm. The right columns of each group show the EC iF.E. values in a flow cell, where CO_2 was supplied by permeating gas through the GDE at a gas flow rate of 20 sccm. Despite the smaller amount of supplied CO_2, EC iF.E. values were higher when using the gas diffusion method. Each point was repeatedly measured three times, and the error bars indicate standard deviation. **b** Schematic depiction of the flow cell components. The components are stacked without gap in a real operation. While 0.5 M TBACl-2-chloroethanol solution cycles through the catholyte path, gas is supplied into the solution by permeating through a Ni-sputtered PTFE film GDE (green arrow). **c** Average indirect Faradaic efficiency values of ethylene carbonate at three different current densities (10, 25, 50 mA/cm^2) and two different compositions of gas (100%, 15% CO_2). The gas was supplied at a gas flow rate of 20 sccm during the electrolysis. EC iF.E. value decreases when the rate of electron supply exceeds the supply of CO_2. Each point was repeatedly measured three times, and the error bars indicate standard deviation. **d** Left axis indicates concentration in the catholyte and indirect Faradaic efficiency values for EC by cell operation time, using 15% CO_2 gas, at a current density of 50 mA/cm^2. EC concentration linearly increases up to 0.09 M during 5 hours of electrolysis. EC iF.E. value maintains around 45%, indicating operational stability. Right axis indicates the overall cell voltage during operation. The voltage was not iR-corrected. Source data for Fig. 4a, c, d are provided as a Source Data file.

HER on chlorohydrins occurs with nearly 100% indirect Faradaic efficiency, the limiting step appears to be the chemical reaction between alkoxides and CO_2, rather than alkoxide formation. In this case, improving CO_2 solubility and diffusivity could be effective strategies. Following this assumption, we introduced acetonitrile as a diluent for chlorohydrins due to its high CO_2 solubility[36,37] and low viscosity[38] (Supplementary Table 2 and 3), diluting until the chlorohydrins' concentrations reached 1.0 M to ensure sufficient reactant availability while leveraging acetonitrile's advantageous properties. Since diffusion coefficients are inversely proportional to the viscosity of the medium, acetonitrile, which has a viscosity one-tenth that of 2-chloroethanol, would have high CO_2 diffusivity. As the gold line indicates (Fig. 5), the corresponding cyclic carbonates were successfully synthesized with significantly enhanced yields, suggesting the expandability and generality of our method. Moreover, in the acetonitrile solvent, both Faradaic efficiency of HER and the indirect Faradaic efficiency of ethylene carbonate production reached near 100%.

The increase in ethylene carbonate production efficiency using acetonitrile was also confirmed with the GDE configuration and 15% CO_2. Specifically, the indirect Faradaic efficiency of ethylene carbonate increased from 46% to 78% (Supplementary Fig. 15) when employing acetonitrile compared to without it. Again, in both cases, the HER Faradaic efficiency was near 100% (Supplementary Fig. 16), suggesting that acetonitrile does not affect the electrochemical reaction but rather the subsequent alkoxide-CO_2 adduction either by its high CO_2 solubility (Supplementary Fig. 17) or low viscosity.

Discussion

In summary, this cascading reaction investigated here offers two key advantages: CO_2 capture through highly selective redox reactions and simultaneous conversion to a value-added chemical without additional processes. HER on 2-chloroethanol occurs with high selectivity, and CO_2-inserted ethylene carbonate is produced through a series of domino reactions. By ensuring the high selectivity in O-H bond deprotonation, maintaining the reactivity of alkoxide intermediates, and enabling efficient mass transfer of CO_2, the process exhibit Faradaic efficiencies of up to 100% for both ethylene carbonate and hydrogen. By introducing gas diffusion electrodes and acetonitrile as a diluent, highly efficient

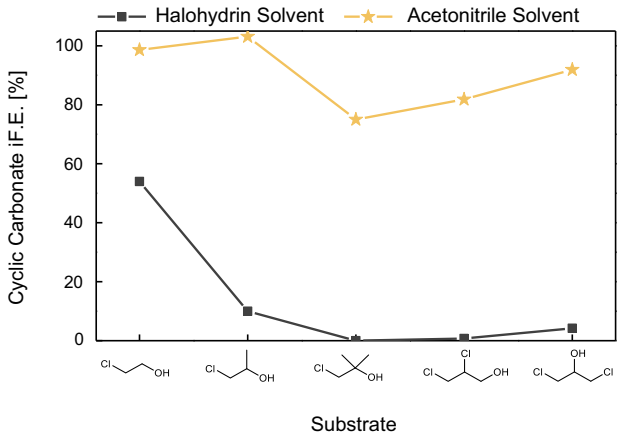

Fig. 5 | Substrate scope for cyclic carbonate electrosynthesis. Average indirect Faradaic efficiency values for the corresponding cyclic carbonate synthesized from five different vicinal halohydrins (2-chloroethanol, 1-chloro-2-propanol, 1-chloro-2-methyl-2-propanol, 2,3-dichloro-1-propanol, 1,3-dichloro-2-propanol). Each substrate underwent reaction either in the halohydrin solvent itself or by adding it as a 1.0 M reactant in acetonitrile solvent. Acetonitrile solvent was used to improve CO_2 mass transportation in the catholyte by decreasing solvent viscosity. Each point was repeatedly measured three times. Source data for Fig. 5 are provided as a Source Data file.

ethylene carbonate production can be achieved even with dilute CO_2 streams. Our system could be further applied to synthesizing various cyclic carbonates from vicinal halohydrins. We envision that this approach of electrochemically activating substrate molecules for CO_2 capture and autonomous conversion will provide a new direction for future carbon capture and utilization (CCU) technologies.

Methods

Chemicals and materials

Reagents were purchased from commercial suppliers and used without further purification. Electrodes included platinum foil (0.025-mm thick, 99.99% metal basis), nickel foil (0.1-mm thick, 99.5% metal basis), gold foil (0.1-mm thick, 99.9975+% metal basis), and glassy carbon plates (3 mm × 25 mm × 25 mm), all purchased from Alfa Aesar. For electrolytes, 2-chloroethanol (99%), 2-bromoethanol (95%), and 2-iodoethanol (99%) were obtained from Sigma Aldrich. Supporting electrolytes included tetrabutylammonium chloride (≥97.0%) and tetramethylammonium chloride (≥97.0%). A hydrochloric salt of 1,8-diazabicyclo[4.3.0]non-5-ene (DBN) was synthesized in lab due to its commercial unavailability. This synthesis involved mixing DBN (purum, ≥98.0%, from Sigma Aldrich) with diethyl ether (99.50%, from DAEJUNG Chemicals & Metals) and adding ethereal HCl solution under vigorous stirring in an inert atmosphere, resulting in a dry white solid after 2 h. The resulting salt was used without further purification. For aqueous electrolytes, high purity deionized (DI) water (18.2 MΩcm) and sodium chloride (99%) from DAEJUNG Chemicals & Metals were used. Anion exchange membranes were sourced from ASTOM (NEOSEPTA-AHA, AFN) and stored in 0.5 M aqueous sodium chloride solution. Specification of anion exchange membranes is provided in Supplementary Table 4. Acetonitrile (99.50%) dried with molecular sieves (3 Å, 1/16 in. rod) was used as the electrolyte solvent in the experiments shown in Figs. 3a, 5, Supplementary Figs. 1, 2, 8, 10 and 11. Both the acetonitrile and molecular sieves were purchased from DAEJUNG Chemicals & Metals.

Preparation of electrodes

1. Metal foil electrodes: Pt, Ni, and Au foil electrodes were used as received. Post-experiment, they were cleaned by sonication in acetone.
2. Gas diffusion electrodes: GDEs were fabricated by sputtering a nickel layer onto PTFE membrane filters (Aspire laminated ePTFE membrane, QL822, Sterlitech Corporation). PTFE membranes were affixed to a 4" silicon wafer using Kapton tape. Nickel layers were sputtered on the polypropylene side using an SRN120 SPUTTER at 500 W RF power for 1402 s, resulting in a 300 nm thickness.
3. Glassy carbon electrodes: Glassy carbon plates (Alfa Aesar, 3 mm × 25 mm × 25 mm) were polished with diamond paste and rinsed with acetone before each use. They were cleaned post-experiment by sonication in acetone.
4. Dimensionally stable anodes (DSA): Dimensionally stable anodes (DSA) were created by brush-coating iridium ink onto titanium plates. The ink was prepared by dissolving $IrCl_4{\cdot}xH_2O$ (≥99.9%, Sigma-Aldrich) in 2-propanol (99%, Sigma-Aldrich). After coating, the electrodes were sintered at 500 °C.

Bulk electrolysis

A membrane-separated cell was used to separate electrolytes with different solvents. Metal foils served as the working electrode; exposed area controlled to 2.25 cm^2 (Supplementary Fig. 18). The catholyte, a liquid halohydrin, served both as a reactant and a solvent to minimize side reactions and included 0.5 M organic salts as a supporting electrolyte. In Fig. 5, acetonitrile (99.50%, from DAEJUNG Chemicals & Metals) dried with molecular sieves was used as the solvent. TBACl was used as the supporting electrolyte unless otherwise noted (Fig. 2c). Electrolytes were prepared immediately before each electrolysis experiment. Argon (99.999%) or CO_2 (99.999%) gas from SINJIN GAS TECH CO. was bubbled into the catholyte for 25 min at 250 sccm before electrolysis. In the anode compartment, an aqueous halide solution and a glassy carbon anode facilitated the halohydrin evolution reaction. Ethylene gas was bubbled into the anolyte during electrolysis at 20 sccm as needed. Bulk electrolysis was performed at various current densities in a two-electrode system, with the cell sealed to prevent gas loss. Gas products were analyzed by gas chromatography after passing 5 C of charge, and liquid products were analyzed by NMR after passing 30 C of charge. Experiments were conducted at room temperature (approximately 25 °C) using a potentiostat. (VSP-300, Bio-Logic Science Instruments).

For the flow cell, a GDE served as the working electrode, and a DSA plate was the counter electrode. Electrodes were masked with gaskets to control the exposed area to 0.42 cm^2 (Supplementary Fig. 18). Liquid flow was driven by a peristaltic pump (EMP-600A) at 5 mL/min, and gas was supplied to the backside of the GDE at 20 sccm during the electrolysis. Bulk electrolysis was conducted at various current densities in a two-electrode system at room temperature using a potentiostat (CHI600). Liquid products were analyzed after passing 30 C of charge.

Product analysis

Gas products were analyzed using a Clarus 580 Gas Chromatography instrument. A 0.1 mL of gas was sampled after electrolysis and injected into the instrument. Calibration curves were generated using a commercial standard gas sample from SINJIN GAS TECH CO., containing H_2, CO, CH_4, C_2H_2, C_2H_4, C_2H_6, with N_2 as the balance (Supplementary Fig. 19). Liquid products were analyzed by NMR spectroscopy using internal standards. After electrolysis, the catholyte was stored in a refrigerator to prevent ethylene oxide loss. Benzyl benzoate (5 mmol, ≥99.0%, Sigma Aldrich) was added as an internal standard, and the solution volume was adjusted to 10 mL with chloroform (99.5%, DAEJUNG Chemicals & Metals). The solution was then mixed with $CDCl_3$ (99.8 atom % D, Alfa Aesar) in a 1:1 ratio and analyzed by NMR. Cyclic carbonates were quantified by comparing peak areas with benzyl benzoate. Indirect Faradaic efficiency was calculated using the

formula:

$$iF.E.\% = \frac{n\ \text{Cyclic carbonate (mol)} \times 96,485\ \left(\frac{C}{mol}\right)}{Q\ (C)} \times 100\% \quad (2)$$

(n: number of moles of product, Q: total charge passed)

Calibration curves generated using lab-prepared standard reference samples are provided in Supplementary Figs. 20, 21.

Measurement of ethylene oxide evolution (Fig. 2d)

40% TBAOH in methanol was purchased from DAEJUNG Chemicals & Metals and 25% TMAOH in methanol were from Sigma Aldrich. These hydroxide solutions were then diluted to a concentration of 0.5 M by adding methanol (HPLC Grade, 99.8+%) from Alfa Aesar. A DBNH·OH methanol solution was prepared by combining 0.5 M DBN with 0.5 M of deionized water in methanol. TBACl, TMACl, and synthesized DBN·HCl salts were prepared in 0.5 M deuterated methanol (CH3OD, ≥99.8 atom % D, Sigma Aldrich). A mixture of 0.6 mL 0.5 M TBACl-CH_3OD solution, 0.2 mL of 0.5 M TBAOH-CH_3OH solution, and 6.7 µL of 2-chloroethanol (equimolar to TBAOH) was analyzed by NMR immediately after mixing. Subsequent measurements were conducted at 1-h intervals for the same sample. The same procedure was followed for TMA and DBNH analogs. For quantification, a commercial ethylene oxide standard reference sample (1.13 M in methanol) was purchased from Sigma Aldrich. A 0.1 mL of commercial ethylene oxide reference was mixed with 0.1 mL of a 0.5 M TBACl-2-chloroethanol solution and 0.6 mL of $CDCl_3$ to resemble the composition of the prepared samples. The corresponding calibration curves are provided in Supplementary Fig. 22.

Linear sweep voltammetry (Fig. 3a)

A three-electrode system included a Pt foil cathode, $Ag/AgNO_3$ reference electrode, and glassy carbon anode. The $Ag/AgNO_3$ reference electrode was prepared in 0.1 M $TBABF_6$ acetonitrile solution by adding 50 mM $AgNO_3$. The reference electrode was calibrated by soaking it in a $AgNO_3$ solution for one day before use. Both catholyte and anolyte used acetonitrile with 0.5 M TBACl. Halohydrin analyte was added at 50 mM to the catholyte. Acetonitrile was dried with molecular sieves, and anion exchange membrane AHA was stored in 0.5 M TBACl-acetonitrile solution to exclude water. Linear sweep voltammetry was conducted using a potentiostat (VSP-300, Bio-Logic Science Instruments) at a scan rate of 10 mV/sec. The recorded potential versus the 50 mM $Ag/AgNO_3$ reference can be converted to the NHE scale by adding +563 mV[39]. The voltage was measured with iR-correction, automatically applied by EC Lab software at 85% of the R.

Data availability

The authors declare that all data supporting the findings of this study are available within the paper and Supplementary Information. Source data are provided with this paper.

References

1. Haszeldine, Stuart R. Carbon capture and storage: how green can black be? *Science* **325**, 1647–1652 (2009).
2. Saeidi, S. et al. Recent advances in CO2 hydrogenation to value-added products — Current challenges and future directions. *Progr. Energy Combust. Sci.* **85**, https://doi.org/10.1016/j.pecs.2021.100905 (2021).
3. Wu, J., Huang, Y., Ye, W. & Li, Y. CO_2 reduction: from the electrochemical to photochemical approach. *Adv. Sci.* **4**, https://doi.org/10.1002/advs.201700194 (2017).
4. Sharifian, R., Wagterveld, R. M., Digdaya, I. A., Xiang, C. & Vermaas, D. A. Electrochemical carbon dioxide capture to close the carbon cycle. *Energy Environ. Sci.* **14**, 781–814 (2021).
5. Rahimi, M., Khurram, A., Hatton, T. A. & Gallant, B. Electrochemical carbon capture processes for mitigation of CO2 emissions. *Chem. Soc. Rev.* **51**, 8676–8695 (2022).
6. Stern, M. C., Simeon, F., Herzog, H. & Hatton, T. A. Post-combustion carbon dioxide capture using electrochemically mediated amine regeneration. *Energy Environ. Sci.* **6**, 2505–2517 (2013).
7. Bravo, J. et al. Optimization of energy requirements for CO2 post-combustion capture process through advanced thermal integration. *Fuel* **283**, 118940 (2021).
8. Legrand, L., Shu, Q., Tedesco, M., Dykstra, J. E. & Hamelers, H. V. M. Role of ion exchange membranes and capacitive electrodes in membrane capacitive deionization (MCDI) for CO2 capture. *J. Colloid Interface Sci.* **564**, 478–490 (2020).
9. Wang, M., Herzog, H. J. & Hatton, T. A. CO2 capture using electrochemically mediated amine regeneration. *Ind. Eng. Chem. Res* **59**, 7087–7096 (2020).
10. Liu, Y., Ye, H. Z., Diederichsen, K. M., Van Voorhis, T. & Hatton, T. A. Electrochemically mediated carbon dioxide separation with quinone chemistry in salt-concentrated aqueous media. *Nat Commun* **11**, 2278 (2020).
11. Ranjan, R. et al. Reversible electrochemical trapping of carbon dioxide using 4,4′-bipyridine that does not require thermal activation. *J. Phys. Chem. Lett.* **6**, 4943–4946 (2015).
12. Wang, C., Liu, H., Li, X. & Zheng, L. Importance of ambient O2 for electrochemical enrichment of atmospheric CO2. *Ind. Eng. Chem. Res* **52**, 2470–2476 (2013).
13. Willauer, H. D., DiMascio, F., Hardy, D. R. & Williams, F. W. Development of an electrolytic cation exchange module for the simultaneous extraction of carbon dioxide and hydrogen gas from natural seawater. *Energy Fuels* **31**, 1723–1730 (2017).
14. Freyman, M. C. et al. Reactive CO2 capture: A path forward for process integration in carbon management. *Joule* **7**, 631–651 (2023).
15. Lee, G. et al. Electrochemical upgrade of CO2 from amine capture solution. *Nat. Energy* **6**, 46–53 (2021).
16. Li, Y. C. et al. CO2 electroreduction from carbonate electrolyte. *ACS Energy Lett.* **4**, 1427–1431 (2019).
17. Xiao, Y. C. et al. Direct carbonate electrolysis into pure syngas. *EES Catal.* **1**, 54–61 (2023).
18. Wang, J. L., He, L. N., Dou, X. Y. & Wu, F. Poly(ethylene glycol): An alternative solvent for the synthesis of cyclic carbonate from vicinal halohydrin and carbon dioxide. *Aust. J. Chem.* **62**, 917–920 (2009).
19. Hirose, T. et al. Economical synthesis of cyclic carbonates from carbon dioxide and halohydrins using K2CO3. *RSC Adv.* **6**, 69040–69044 (2016).
20. Khokarale, S. G. & Mikkola, J. P. Metal free synthesis of ethylene and propylene carbonate from alkylene halohydrin and CO2 at room temperature. *RSC Adv.* **9**, 34023–34031 (2019).
21. Reithofer, M. R., Sum, Y. N. & Zhang, Y. Synthesis of cyclic carbonates with carbon dioxide and cesium carbonate. *Green. Chem.* **15**, 2086–2090 (2013).
22. Lyubimov, S. E. et al. A simple synthesis of ethylene carbonate from carbon dioxide and 2-chloroethanol using silica gel as a catalyst. *Appl. Catal. A Gen.* **592**, 117433 (2020).
23. Jang, J. H. et al. Electrochemically initiated synthesis of ethylene carbonate from CO2. *Nat. Synth.* **3**, 846–857 (2024).
24. Medvedev, J. J., Medvedeva, X. V., Li, F., Zienchuk, T. A. & Klinkova, A. Electrochemical CO2 fixation to α-methylbenzyl bromide in divided cells with nonsacrificial anodes and aqueous anolytes. *ACS Sustain Chem. Eng.* **7**, 19631–19639 (2019).
25. Peterson, A. A. & Nørskov, J. K. Activity descriptors for CO 2 electroreduction to methane on transition-metal catalysts. *J. Phys. Chem. Lett.* **3**, 251–258 (2012).
26. Back, S., Kim, J. H., Kim, Y. T. & Jung, Y. Bifunctional interface of Au and Cu for improved CO2 electroreduction. *ACS Appl Mater. Interfaces* **8**, 23022–23027 (2016).

27. Chang, C. Y. et al. Sustainable synthesis of epoxides from halohydrin cyclization by composite solid-based catalysts. *Ind. Eng. Chem. Res* **61**, 9970–9980 (2022).
28. Boschloo, G. & Hagfeldt, A. Characteristics of the iodide/triiodide redox mediator in dye-sensitized solar cells. *Acc. Chem. Res.* **42**, 1819–1826 (2009).
29. Andrieux, C. P., Gallardo, I., Savaent, J. M. & Su, K. B. Dissociative electron transfer. Homogeneous and heterogeneous reductive cleavage of the carbon-halogen bond in simple aliphatic halides. *J. Am. Chem. Soc.* **108**, 638–647 (1986).
30. Wang, X. & Song, C. Carbon capture from flue gas and the atmosphere: a perspective. *Front. Energy Res.* **8**, https://doi.org/10.3389/fenrg.2020.560849 (2020).
31. Webster, D. C. & Crain, A. L. Synthesis and applications of cyclic carbonate functional polymers in thermosetting coatings. *Progr. Organic Coatings*. **40**, 275–282 (2000).
32. Gennen, S., Grignard, B., Tassaing, T., Jérôme, C. & Detrembleur, C. CO_2-sourced α-alkylidene cyclic carbonates: a step forward in the quest for functional regioregular poly(urethane)s and poly(-carbonate)s. *Angew. Chem.* **129**, 10530–10534 (2017).
33. Shaikh, A.-A. G. & Sivaram, S. Organic carbonates. *Chem. Rev.* **96**, 951–976 (1996).
34. Schäffner, B., Schäffner, F., Verevkin, S. P. & Börner, A. Organic carbonates as solvents in synthesis and catalysis. *Chem. Rev.* **110**, 4554–4581 (2010).
35. Su, C. C. et al. Cyclic carbonate for highly stable cycling of high voltage lithium metal batteries. *Energy Storage Mater.* **17**, 284–292 (2019).
36. Fogg, P. G. T. *Carbon dioxide in non-aqueous solvents at pressures less than 200 KPA* (Pergamon Press, 1992).
37. Gennaro, A., Isse, A. A. & Vianeuo, E. Solubility and Electrochemical Determination Dipolar Aprotic Solvents of CO, in Some. *J. Electroanal. Chem*. **289**, 203–215 (1990).
38. Marrero, J. & Gani, R. Group-Contribution Based Estimation of Pure Component Properties. *Fluid Phase Equilibria* **183–184**, 183–208 (2001).
39. Pavlishchuk, V. V. & Addison, A. W. Conversion constants for redox potentials measured versus different reference electrodes in acetonitrile solutions at 25 °C. www.elsevier.nl/locate/ica (2000).

Acknowledgements

This research was supported by the Nano & Material Technology Development Program through the National Research Foundation of Korea (NRF) funded by Ministry of Science and ICT(RS-2024-00409405), and the DACU program through the National Research Foundation of Korea(NRF) grant funded by the Korea government(MSIT) (No. RS-2023-00259920). KTN appreciates the support from Institute of Engineering Research, Research Institute of Advanced Materials (RIAM) and Soft Foundry at Seoul National University. We acknowledged an administrative support from SOFT foundry institute.

Author contributions

K.T.N., J.H.K., Y.I. J. and J.H.J. designed the research. J.H.K., and J.H.J. wrote the manuscript. J.H.K., Y.I.J., J.H.J., J.E.K., and H.J.K conducted electrochemical experiments and optimized the conditions for ethylene carbonate synthesis. J.H.K., Y.I.J., J.H.J., J.B.Y., and M.Y.L. investigated vicinal halohydrins for cyclic carbonate synthesis. J.H.K., Y.I.J., J.H.J., and H.J.Y. fabricated the gas diffusion electrode (GDE) and conducted electrochemical experiments using the GDE. All authors contributed to discussions on the experiments and to the writing of this manuscript. K.T.N. guided all aspects of the research.

Competing interests

The authors declare no competing interests.

Additional information

Supplementary information The online version contains supplementary material available at https://doi.org/10.1038/s41467-025-60354-8.

Correspondence and requests for materials should be addressed to Ki Tae Nam.

Peer review information *Nature Communications* thanks the anonymous, reviewer(s) for their contribution to the peer review of this work. A peer review file is available.